Available online at www.sciencedirect.com

SCIENCE DIRECT®

Earth and Planetary Science Letters 227 (2004) 313–330

EPSL

www.elsevier.com/locate/epsl

Detrital geochronology and geochemistry of Cretaceous–Early Miocene strata of Nepal: implications for timing and diachroneity of initial Himalayan orogenesis

P.G. DeCelles[a,*], G.E. Gehrels[a], Y. Najman[b], A.J. Martin[a], A. Carter[c], E. Garzanti[d]

[a]*Department of Geosciences, University of Arizona, Tucson, AZ 85721, USA*
[b]*Department of Environmental Science, Lancaster University, LA1 4YQ, UK*
[c]*School of Earth Sciences, University and Birkbeck College, Gower Street, London WC1E 6BT, UK*
[d]*Dipartimento di Scienze della Terra, Via Mangiagalli, 34-20133 Milano, Italy*

Received 12 May 2004; received in revised form 17 August 2004; accepted 27 August 2004
Editor: K. Farley

Abstract

The onset of mountain building in the western part of the Himalayan orogenic belt has been documented in the synorogenic stratigraphic record of northern Pakistan and India as Early to Middle Eocene (~52 Ma). Eocene strata in the Tethyan portion of the central part of the Himalayan orogenic belt consist of shallow marine carbonate rocks that lack evidence for initial Himalayan orogenesis, thus leaving open the possibility that the onset of orogeny was significantly diachronous along strike. We report U–Pb ages of detrital zircons and Nd-isotopic and trace element data from associated mudrocks in Cretaceous–Paleocene(?), Eocene, and lower Miocene strata of the southern Lesser Himalayan zone of central Nepal. The Cretaceous–Paleocene(?) Amile Formation is dominated by zircons with Archean–Early Proterozoic U–Pb ages. An abrupt influx of Cambrian–Ordovician and Middle to Late Proterozoic zircons marks the transition into the Eocene Bhainskati Formation, and indicates the onset of erosion of Tethyan rocks in the nascent Himalayan thrust belt. An increased proportion of Late Proterozoic zircons in fluvial litharenites of the lower Miocene Dumri Formation signals initial erosion of Greater Himalayan protoliths. The Nd-isotopic and trace element data support the unroofing history documented by the U–Pb zircon ages. The fact that middle Eocene strata in Nepal were derived from the Himalayan thrust belt reduces the maximum time lag between the onset of orogenesis in the northwest and central Himalaya to no more than ~2 My.

Keywords: Himalaya; collision orogeny; sediment province; detrital zircons; Nd-isotopes

* Corresponding author. Tel.: +1 520 621 4910; fax: +1 520 621 2672.
E-mail addresses: decelles@geo.arizona.edu (P.G. DeCelles), gehrels@geo.arizona.edu (G.E. Gehrels), y.najman@lancaster.ac.uk (Y. Najman), amartin@geo.arizona.edu (A.J. Martin), a.carter@ucl.ac.uk (A. Carter), eduardo.garzanti@unimib.it (E. Garzanti).

0012-821X/$ - see front matter © 2004 Elsevier B.V. All rights reserved.
doi:10.1016/j.epsl.2004.08.019

1. Introduction

Provenance analysis of clastic sedimentary rocks has traditionally relied upon petrographic data sets from sandstones [1]. In regions where source terranes vary considerably in age and contain rocks that may yield geochronologic information, isotopic methods have been employed to assess sediment provenance [2–6]. The use of U–Pb ages of detrital zircon grains has proven valuable in geochronologic provenance studies because zircons are chemically stable and mechanically durable in weathering and depositional environments. Detrital zircon U–Pb ages may provide the only reliable means of assessing provenance in compositionally ultrastable sands and sandstones [7].

The early history of erosion of the Himalayan orogenic belt (Fig. 1) presents a problem that is well suited to a combined geochronological and geochemical provenance study. Plate reconstructions and stratigraphic data sets suggest that initial collision between the Indian and Eurasian plates occurred in northern India between latest Paleocene and earliest Eocene time (~55–51 Ma [8–11]). Lower Eocene foreland basin deposits in northern India (Zanskar) and Pakistan contain clear-cut petrographic and trace element evidence for erosion of source terranes in the Indus suture zone and the northern Himalayan thrust belt [10–13]. In contrast, the Eocene section of the Tethyan Himalaya north of Mount Everest (Zhepure Mountain area, Fig. 1) consists of shallow marine carbonates [14,15] and the foreland basin record farther south in Nepal contains no obvious petrographic evidence of erosional unroofing of Himalayan source terranes until Early Miocene time [16] (Figs. 2 and 3). The Eocene of Nepal consists of ~90–150 m of black shale, fine-grained quartz arenite, and limestone that accumulated in shallow marine environments [17,18]. If the Eocene sections in Nepal and southern central Tibet (Zhepure Mountain area [14]) are indeed pre-collisional, then the possibility of a significantly time-transgressive, eastward propagating collision remains viable [8,15], with potential implications for total shortening and convergence estimates in the Himalayan orogenic belt.

Previous work hints at the possibility that Eocene strata in Nepal are actually composed in part of sediments derived from the nascent Himalayan thrust belt. Neodymium isotopic data from Nepal [6] indicate that Eocene strata were derived partly from relatively juvenile sources, perhaps located in the arc and forearc region; however, these data by themselves cannot rule out a juvenile source in peninsular India, such as the mid-Cretaceous Rajmahal basalts. The interpretation that Eocene rocks in Nepal are synorogenic deposits hinges entirely upon a small (only 18 grains) U–Pb detrital zircon data set that indicates a change from dominantly Early Proterozoic and Archean ages (between 1856 and 2562 Ma) in upper Cretaceous–Paleocene(?) strata to a mix of ages ranging between Archean and Early Cambrian (between 2446 and 531 Ma) in Eocene strata [16]. In this paper, we bolster previous interpretations of the provenance of Cretaceous through lower Miocene sedimentary rocks in the Nepalese Himalayan thrust belt with 775 U–Pb detrital zircon ages, nine Nd-isotopic analyses, and trace element data from 15 samples spanning the Cretaceous–Miocene transition. Our results firmly establish that the source of sediment in northern Greater India shifted from mainly southerly (cratonal) to northerly (from the growing Himalayan thrust belt) during Early Eocene time.

2. Geologic and tectonic setting

The Himalayan thrust belt consists of four tectonostratigraphic zones that are separated by orogen-wide fault systems (Fig. 1) [19]. The northern zone is referred to as the Tibetan Himalayan zone (THZ) and consists of a thick succession of folded and thrust faulted [20–23] Paleozoic through Eocene carbonate and fine-grained clastic rocks of the Tethyan sequence [24–29]. Tethyan strata were deposited along the northern margin of Indian Gondwanaland prior to, during, and immediately after its extensional break-up [26,27]. A belt of domal uplifts cored by medium- to high-grade metamorphic rocks runs the length of the medial part of the THZ [20,30]. The northern boundary of the THZ is the Indus-Yarlung suture zone, which marks the former subduction zone between the Indian and Eurasian plates. The THZ is separated from the Greater Himalayan zone (GHZ) by the South Tibetan detachment system, a top-to-the-north, normal-sense fault system [31–35].

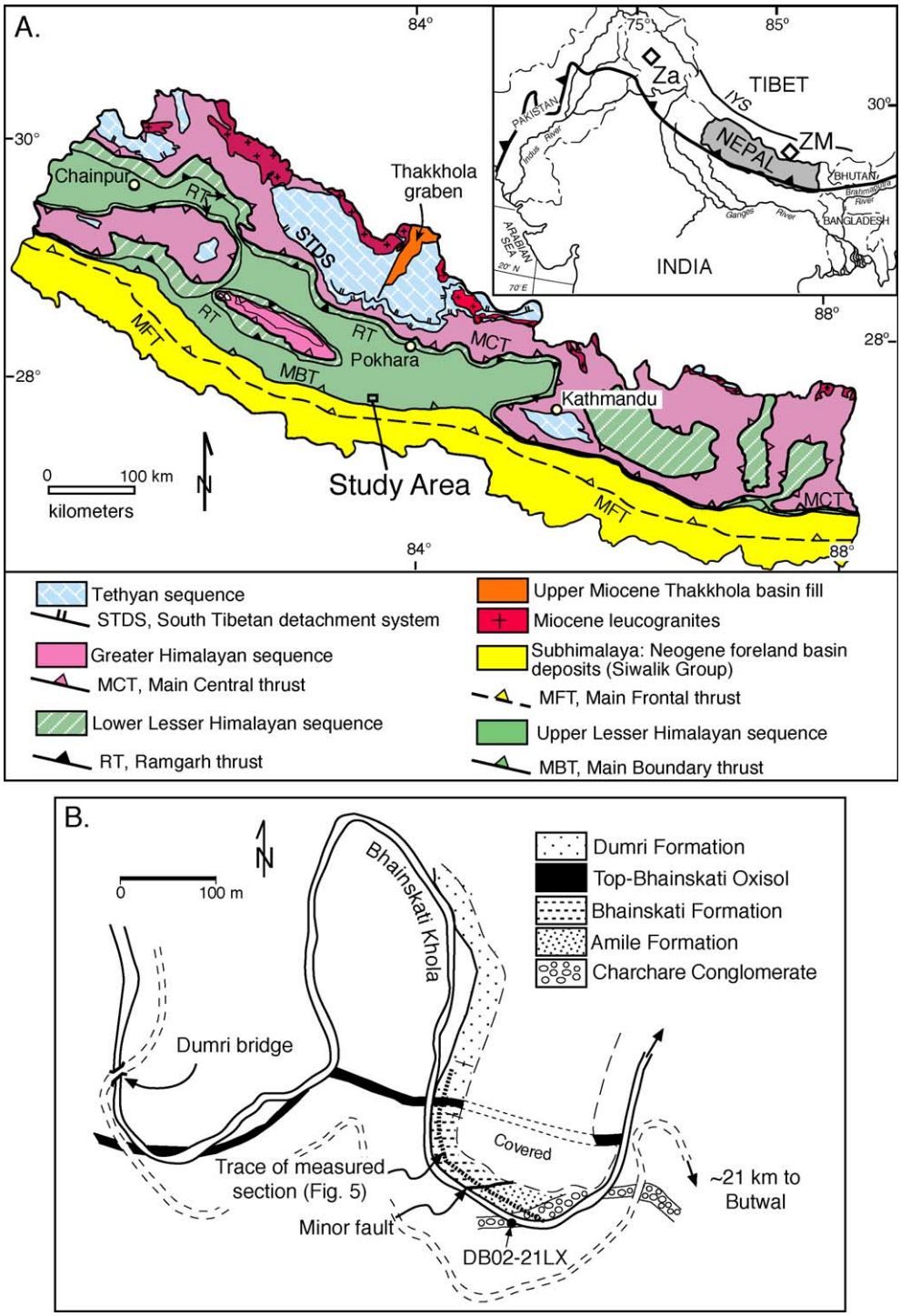

Fig. 1. (A) Generalized geologic map of Nepal, modified from [91] according to [35,59]. Box indicates location of study area in central Nepal. Inset shows setting of Nepal in the center of the Himalayan orogenic belt (barbed line) and locations of Zanskar (Za) and Zhepure Mountain (ZM). IYS is trace of Indus-Yarlung suture. (B) Detailed map of the sample collection area near Dumri bridge along Bhainskati Khola on the Pokhara-Butwal road in central Nepal.

The GHZ comprises amphibolite-grade metasedimentary and meta-igneous rocks of the Greater Himalayan sequence [32,34,36]. In much of Nepal, the Greater Himalayan sequence has a simple three-member tectonostratigraphy [24,35]. Formation I mainly consists of pelitic schist and paragneiss; Formation II is composed of a mixture of calcsilicate gneiss and paragneiss; and Formation III consists of orthogneiss bodies that intrude Formation II. In the southernmost erosional outliers of Greater Himalayan rocks, granitic mylonites and undeformed granites of Cambrian–Ordovician age [29,32,37–43] are probable equivalents of Formation III orthogneisses. Large bodies of Early Miocene leucogranite are present in the upper part of the GHZ [32,35,44–46]. The southern boundary of the GHZ is marked by the Main Central thrust, which is given local names where it bounds erosional outliers of the GHZ.

The Main Central thrust juxtaposes Formation I with greenschist- to lower amphibolite-grade metasedimentary rocks of the Lesser Himalayan zone (LHZ) along a major shear zone (e.g., [47]). Recent studies have shown that the Nd-isotopic compositions and U–Pb detrital zircon ages of Greater and Lesser Himalayan rocks differ markedly [6,42,48–52]. These isotopic and geochronologic differences provide a means of recognizing the protolith boundary between the GHZ and LHZ as well as their silicilastic erosional byproducts in Himalayan synorogenic sediments [5,6,42,51,53,54]. In Nepal, the Lesser Himalayan zone includes three lithostratigraphic units: the Lesser Himalayan sequence, of Proterozoic age; the Gondwana sequence, of Permian through Paleocene age; and the Eocene–lower Miocene deposits that are addressed in this paper [55]. The Lesser Himalayan sequence includes quartzite, phyllite, slate, dolostone, limestone (locally chert-bearing), amphibolite, and intrusive bodies of granitic augen gneiss (e.g., the Ulleri augen gneiss) [55,56].

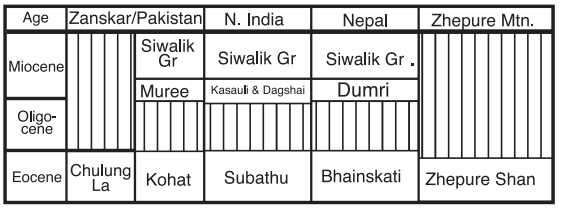

Fig. 2. Chart showing Tertiary stratigraphy in the Himalayan foreland and hinterland, after [10,16].

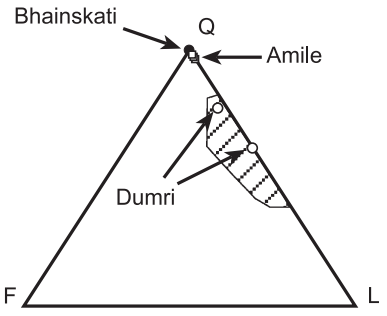

Fig. 3. Ternary quartz-feldspar-lithic grain (QFL) diagram showing modal framework grain compositions of individual samples from this study (symbols) and previous work. Cross-hatched area represents range of Dumri sandstone compositions documented in [16].

The Gondwana sequence includes sandstone, shale, coal, and minor limestone [17]. The Eocene–lower Miocene deposits are described below. The southern boundary of the LHZ is the Main Boundary thrust. Other important structures in the LHZ are the Ramgarh thrust and the Lesser Himalayan duplex [57–60].

The Subhimalayan zone is the frontal part of the thrust belt and consists of several imbricate thrust-bounded panels of Neogene fluvial sandstone, siltstone, and conglomerate of the Siwalik Group. The Siwalik Group constitutes the proximal foredeep and wedge-top portions of the Himalayan foreland basin system [41,61].

3. Zircon ages from Himalayan tectonostratigraphic zones and Northern India

Rocks of the THZ, GHZ, and LHZ are easily distinguished by the contrasting U–Pb ages of their detrital (i.e., recycled) and primary igneous zircons (Fig. 4; [42,43]). Lesser Himalayan detrital zircons have age distribution peaks centered on ~1850 and ~2500 Ma. Igneous rocks in the Lesser Himalayan sequence (Ulleri augen gneiss and intermediate fine-grained metavolcanic rocks) yield zircons with ages between ~1830 and ~1967 Ma. Greater Himalayan detrital zircon ages are broadly clustered about 1100 Ma, with lesser peaks at ~1500–1700 and ~2500 Ma. Singh et al. [62] reported ~823 Ma zircon ages from igneous rocks in the GHZ of northern India. The youngest detrital zircons from Greater Himalayan rocks are approximately 680 Ma. Granitic gneisses in

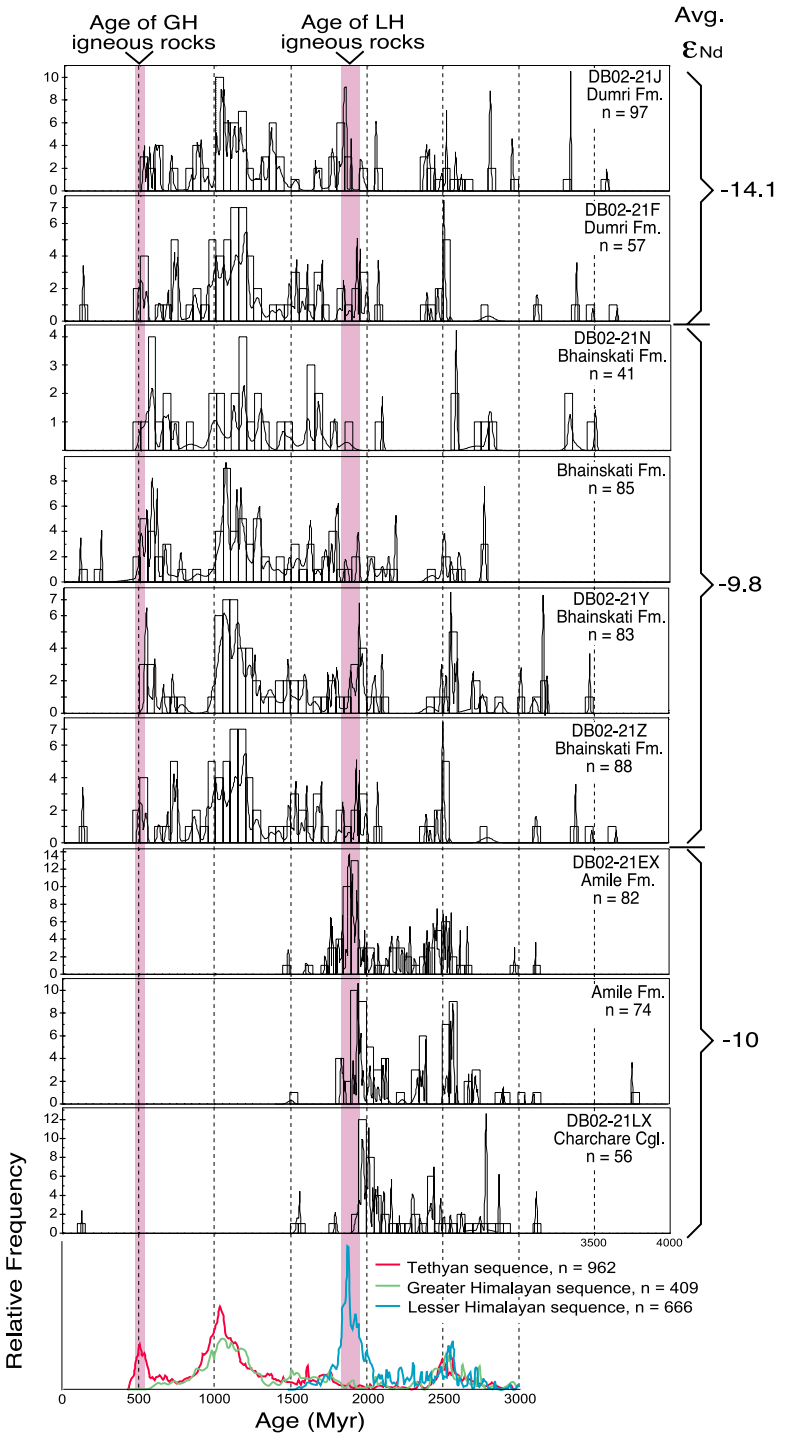

Fig. 4. U–Pb relative age probability diagrams (using the program of Ludwig [81]) from Himalayan tectonostratigraphic terranes (bottom panel) and Late Cretaceous–Early Miocene strata of south-central Nepal. The pink bars indicate age ranges of igneous rocks in Lesser Himalayan sequence (~1850 Ma) and Greater Himalaya (~500 Ma). On the right are ε_{Nd} values of floodplain siltstones from this paper and [6].

Formation III and undeformed granites in the erosional outliers of the GHZ yield zircons with ages of ~470–490 Ma [39–41,43,63,64]. Similar granitoid rocks in the north Himalayan domes (notably the Kangmar dome) yield ages of ~510 Ma [30]. The High Himalayan leucogranites contain zircons that produce discordant ages interpreted to be a result of Early Miocene overgrowths on inherited early Paleozoic cores [32,48]. Detrital zircons from the Tethyan sequence have ages that are similar to those of GHZ detrital zircons, with the addition of a younger population of ~500 Ma grains [43].

In addition to providing a valuable zircon provenance tool in the Himalayan foreland basin deposits, the U–Pb ages constrain the ages of the Greater and Lesser Himalayan tectonostratigraphic terranes [42,43]. The metasedimentary rocks of the Lesser Himalayan zone are most likely Early Proterozoic (~1850–1500 Ma), and Greater Himalayan sedimentary protoliths are bracketed between Late Proterozoic and Late Cambrian. These chronological interpretations are consistent with Nd-isotopic data that suggest greater antiquity for the Lesser Himalayan sequence in Nepal [6,48–51,54].

Crustal ages in India and surrounding regions of Gondwanaland (including Africa, Arabia, Australia, and East Antarctica) can be grouped as follows [65,66]: (1) Archean (>2.5 Ga) crust is widespread in India, central-eastern Africa (including Madagasgar), and western Australia. (2) Late Archean–Early Proterozoic (~2.6–1.8 Ga) crust is present in northern Australia, northern India, eastern Africa, and locally in the Arabia–Nubia shield. (3) Early to Middle Proterozoic (1.8–1.0 Ga) crust is most prevalent in the Eastern Ghats along the east coast of India, in the Singhbhum craton of northern India, eastern Africa, and in East Antarctica. (4) Late Proterozoic (1.0–0.6 Ga) crust is widespread in eastern Africa, Arabia–Nubia, and along the eastern coast of India. (5) Early Cretaceous magmatic activity was widespread from southeastern Africa to northern India and western Australia, and Cretaceous sandstones in the THZ are rich in volcaniclastic detritus [28]. Cretaceous igneous rocks are also common in the Gangdese magmatic arc and forearc directly north of the Indus suture zone.

From the distribution of crustal ages, it may be inferred that: Archean detrital zircons in Lesser, Greater, and Tibetan Himalayan rocks have their ultimate sources mainly in peninsular India and possibly western Australia; Early Proterozoic detrital zircons, the signature of Lesser Himalayan rocks, were probably derived from northern India and igneous rocks that are widely represented in Lesser Himalayan strata (Fig. 4); Middle Proterozoic grains could have been derived from the Eastern Ghats, northern India, eastern Africa, and possibly East Antarctica; Late Proterozoic zircons were derived mainly from the Arabia–Nubia shield and the East African orogenic belt, which was part of the broader Pan-African orogenic system; and the Cambrian–Ordovician zircons that are typical of post-Cambrian Tethyan strata were most likely derived from late Pan-African granites that are widespread in the Greater Himalayan zone, such as the orthogneisses of Formation III and the granites of the southern structural outliers of the Greater Himalayan sequence. Cretaceous zircons would have been available from young igneous rocks in northeastern India (Rajmahal Hills, ~115–120 Ma [67]), from recycled sources in Cretaceous strata of the THZ, and from the Indus suture zone (~120–50 Ma [68,69]). Therefore, it can be postulated that Himalayan pre-orogenic sediments of Nepal should be dominated by Archean and Early Proterozoic detrital zircons reflecting a southerly, Indian provenance. Early synorogenic sediments should contain abundant Late Proterozoic grains, reflecting erosion of Tethyan and possibly Greater Himalayan rocks and a switch to northerly provenance. With continued erosion of the rising Himalaya, the abundance of Early Proterozoic zircons (recycled from Lesser Himalayan strata) should increase. Cretaceous zircons provide ambiguous provenance information, inasmuch as these could be derived from northern India, Cretaceous sandstones in the THZ, and the Indus-Yarlung suture zone.

4. Stratigraphic context

We address the timing of the transition from pre-collisional to syn-collisional sedimentation along the southern side of the Himalayan orogenic belt by analyzing detrital zircon U–Pb ages, Nd isotopes, and trace element compositions of upper Cretaceous through lower Miocene strata in the frontal part of the thrust belt in Nepal. Stratigraphic sections of the critical

transition from the Gondwana sequence to the Miocene are located in central Nepal, where Sakai [17,70] has provided detailed sedimentological and biostratigraphic descriptions of the units (Figs. 1B and 5).

The Eocene–lower Miocene section rests above strata that are assigned to the Upper Gondwana series [17], including the Amile and Taltung Formations (Fig. 5). The Taltung Formation (including the Charchare Conglomerate) consists of 200–250 m of coarse-grained, volcaniclastic sandstone and conglomerate deposited by northwestward flowing fluvial channels [18,70]. Overlying the Taltung Formation is the Amile Formation, which consists of approximately 50–200 m of massive white quartz arenite (Figs. 3 and 5), carbonaceous shale, quartzose pebbly sandstone, lignite, and coal. Sakai [17] reported thin, fossiliferous, marine siltstone and carbonate layers. The upper Amile Formation is overlain abruptly by black, organic-rich, marine shale and interbedded very fine-grained to granular quartzose sandstone and fossiliferous limestone beds (Fig. 5). We place the base of the Bhainskati Formation at the change from thick quartzose sandstone to marine black shale. The Amile Formation in the sampled section is bounded by faults, and probably not representative of the typical Amile thickness. The Bhainskati Formation is ~90 m thick [17]. The upper several tens of meters of the Bhainskati Formation contain oolitic ironstone layers, and a several-meters-thick, mottled, kaolinitic and hematitic Oxisol layer caps the formation [16]. Resting abruptly above the Oxisol are medium-grained, lithic-rich sandstones and siltstones of the ~800–1200-m-thick Dumri Formation. The Dumri contains channel, floodplain, and paleosol facies that were deposited by generally southwestward flowing fluvial systems [16].

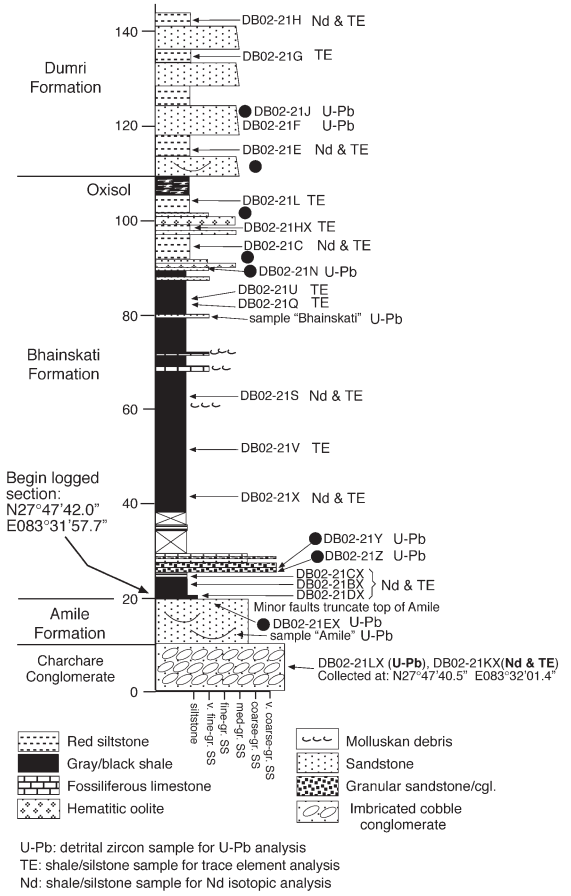

Fig. 5. Log of measured stratigraphic section of the Cretaceous–lower Miocene section of south-central Nepal, showing sample locations. Black circles represent locations of samples used in modal petrographic analysis (Fig. 3).

Chronostratigraphic control on the Cretaceous–Early Miocene section in Nepal is based on a combination of biostratigraphy, magnetostratigraphy, and radiometric dating. The Taltung Formation is reported to contain Late Jurassic–Early Cretaceous plant fossils, and together with the Aulis basalt is correlated with the Rajmahal and Jabalpur Series in Peninsular India [17]. The Rajmahal basalts have yielded whole rock and single crystal K–Ar and $^{40}Ar/^{39}Ar$ ages of 115–118 Ma [67,71,72]. Our sample from the Charchare Conglomerate yielded a single detrital zircon with a $^{206}Pb/^{238}U$ age of 125±1 Ma, which provides a maximum age for the Taltung Formation. Sakai et al. [73] reported an Rb–Sr mineral isochron age of 96.7±2.8 Ma from the Aulis Basalt member of the Taltung Formation. The age of the Amile Formation can be bracketed only loosely between Early Cretaceous and Early Eocene time [17]. This is consistent with the geochronological evidence discussed above concerning the underlying Taltung Formation, as well as $^{206}Pb/^{238}U$ ages of 118±2 and 120±2 Ma obtained in our previous analysis of detrital zircons in the Amile Formation [16].

The Bhainskati Formation in central Nepal is considered to be Middle to Late Eocene on the basis of abundant foraminifera and other marine fossils [17]. However, the lower half of the formation in central Nepal has not been dated. Fuchs and Frank [74]

reported a paleontological age of Late Paleocene–Early Eocene for the equivalent Subathu Formation in western Nepal. Mathur [75] established a Late Paleocene–early Middle Eocene age for the Subathu Formation in northern India. The ages of the Dumri Formation and its northern Indian lithostratigraphic equivalents (the Kasauli and Dagshai Formations) are not well documented. These units have yielded detrital mica $^{40}Ar/^{39}Ar$ ages as young as ~20–22 Ma [5,59,76], providing a maximum age for the unit as a whole. Unpublished magnetostratigraphic data from western Nepal suggest that the Dumri ranges between ~20 and 15 Ma (Ojha et al., unpublished data).

5. Methods

5.1. U–Pb geochronologic analyses of zircon by laser-ICPMS

U–Pb geochronology of zircons was conducted by laser ablation multicollector inductively coupled plasma mass spectrometry (LA-MC-ICPMS). The analyses involve ablation of zircon with a New Wave DUV193 Excimer laser (operating at a wavelength of 193 nm) using a spot diameter of 15, 25, 35, or 50 μm, depending on zircon grain size. The ablated material is carried in argon gas into the plasma source of a Micromass Isoprobe, which is equipped with a flight tube of sufficient width that U, Th, and Pb isotopes are measured simultaneously. All measurements are made in static mode, using Faraday detectors for ^{238}U, ^{232}Th, $^{208–206}Pb$, and an ion-counting channel for ^{204}Pb. Ion yields are ~1 mV/ppm. Each analysis consists of one 30-s integration on peaks with the laser off (for backgrounds), 20 1-s integrations with the laser firing, and a 30-s delay to purge the previous sample and prepare for the next analysis. The ablation pit is ~20 μm deep.

Common Pb correction is made by using the measured ^{204}Pb and assuming an initial Pb composition from Stacey and Kramers [77] (with uncertainties of 1.0 for $^{206}Pb/^{204}Pb$ and 0.3 for $^{207}Pb/^{204}Pb$). Our measurement of ^{204}Pb is unaffected by the presence of ^{204}Hg because backgrounds are measured on peaks (thereby subtracting any background ^{204}Hg and ^{204}Pb), and because very little Hg is present in the argon gas.

Inter-element fractionation of Pb/U is generally ~15%, whereas fractionation of Pb isotopes is generally <5%. In-run analysis of fragments of a large zircon crystal (generally every fifth measurement) with known age of 564±4 Ma (2-sigma error) (Gehrels, unpublished data) is used to correct for this fractionation.

Fractionation also increases with depth into the laser pit by up to 5%. The accepted isotope ratios are accordingly determined by least-squares projection through the measured values back to the initial determination. Analyses that display >10% change in ratio during the 20-s measurement are interpreted to be variable in age (or perhaps compromised by fractures or inclusions), and are excluded from further consideration.

The measured isotopic ratios and ages are reported in Table 1. Errors that propagate from the measurement of $^{206}Pb/^{238}U$, $^{206}Pb/^{207}Pb$, and $^{206}Pb/^{204}Pb$ are reported at the 1-sigma level. Additional errors that affect all ages include uncertainties from U decay constants, calibration correction, age of the calibration standard, and composition of common Pb.

Age interpretations for these analyses are complicated by the known occurrence in the region of inheritance in zircons from ~500 Ma granitoids combined with early Paleozoic and Tertiary Pb-loss (or new zircon growth) in >1.0 Ga detrital zircons. This produces discordant analyses in the 500- to 1000-Ma age range that are of uncertain crystallization age. An additional factor that complicates analyses in this age range is the change in precision of $^{206}Pb/^{238}U$ and $^{206}Pb/^{207}Pb$ ages–$^{206}Pb/^{238}U$ ages are generally more precise for younger ages whereas $^{206}Pb/^{207}Pb$ ages are more precise for older ages. Fortunately, patterns of discordance by Pb loss (or young zircon growth) are recognizable on Pb/U concordia diagrams as an array of analyses that project from a >1.0-Ga upper intercept to a young lower intercept (e.g., Fig. 6; sample DB02-21EX). Our strategy in interpreting ages is accordingly as follows: (1) For samples that display discordia patterns suggestive of Pb loss (and/or growth of young zircon), we use $^{206}Pb/^{207}Pb$ ages and rely only on analyses that are less than 30% discordant. (2) For samples that contain a cluster of analyses with concordant to slightly discordant $^{206}Pb/^{238}U$ ages of ~500 Ma (e.g., Fig. 6, sample DB02-21F), we rely on

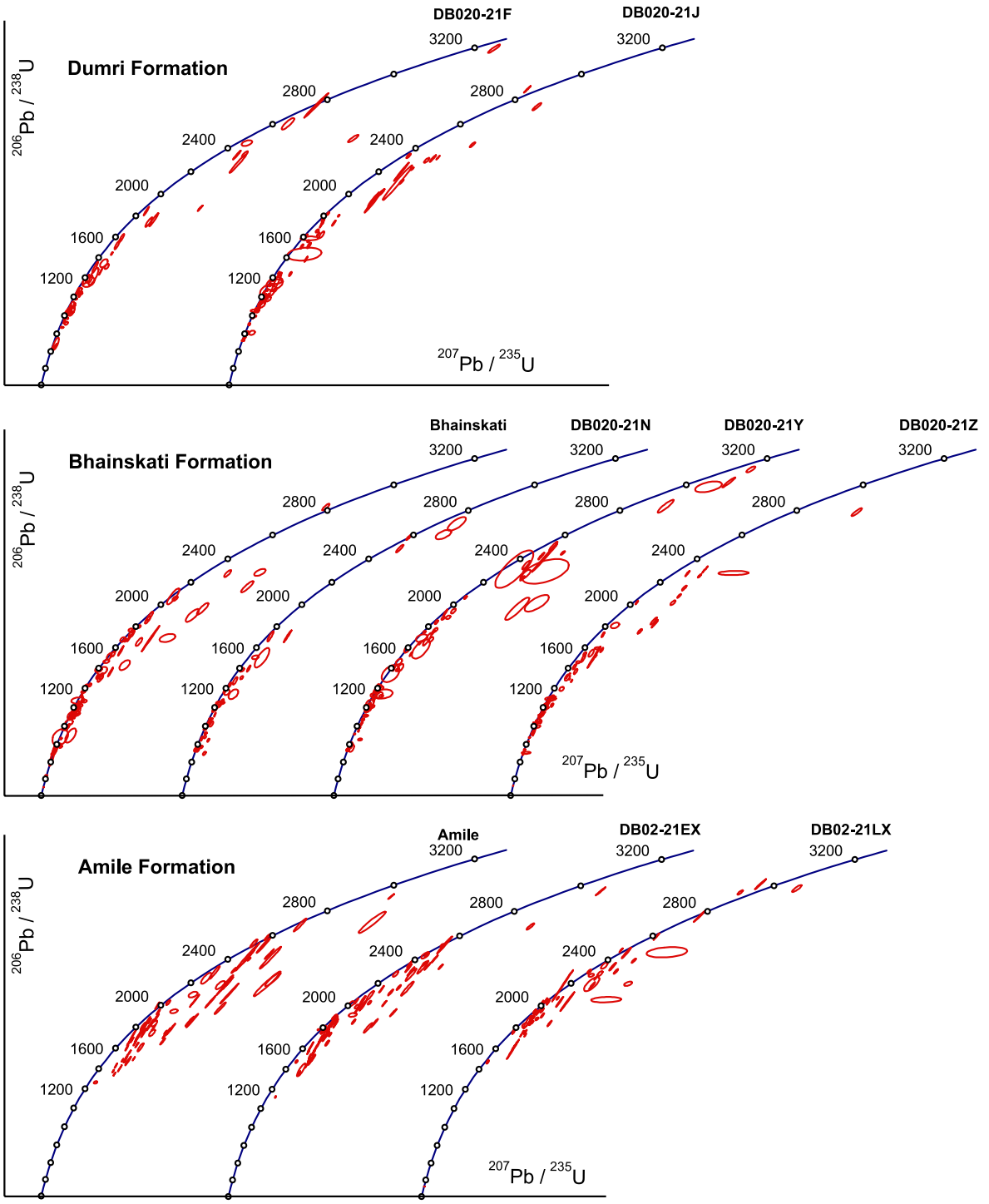

Fig. 6. Pb/U concordia diagrams for Cretaceous–lower Miocene detrital zircon samples from this study. Error ellipses are shown for 1-sigma level of uncertainty, and only analyses that are less than 30% discordant are shown. See text for discussion.

$^{206}Pb/^{238}U$ ages up to 750 Ma and $^{206}Pb/^{207}Pb$ ages if the $^{206}Pb/^{238}U$ ages are >750 Ma.

Detrital zircons were separated from seven new samples of the Charchare Conglomerate (one sample), Amile Formation (one sample), Bhainskati Formation (three samples), and Dumri Formation (two samples). We also analyzed additional grains from the Amile and Bhainskati samples that were used in our previous work [16]. Analyses that yielded isotopic data of acceptable discordance, in-run fractionation, and precision are shown in boldface in Table 1. A total of 775 new zircon ages are reported here, of which 663 are <30% discordant and considered reliable. These analyses are shown on Pb/U concordia diagrams (Fig. 6) and the accepted ages are plotted on relative age-probability diagrams (Fig. 4). Each of these curves is constructed by summing the probability distributions of all grains analyzed from a sample. Age peaks on these diagrams are considered robust if defined by several analyses, whereas less significance is attributed to peaks defined by single analyses because single ages (even if concordant) may not be reliable indicators of crystallization age.

5.2. Nd-isotopic data

Nine samples of siltstone and black shale from the Charchare Conglomerate, Bhainskati Formation, and Dumri Formations were collected for Sm–Nd isotopic analysis (see Fig. 5 for sample locations). Sample size was 0.5 kg. Each sample was crushed in a steel jaw crusher and powdered in an agate-lined shatter box. Approximately 300 mg of powder were dissolved and Sm and Nd isotopes were analyzed following the procedures in [78], except that Sm and Nd were loaded on Ta side filaments for mass spectrometry. Although most samples contained graphite, concentrations were low enough to not interfere with dissolution of the non-graphite portion of the sample. We used a ^{149}Sm–^{150}Nd tracer to determine element abundances, and Nd isotopic measurements were normalized to $^{146}Nd/^{144}Nd=0.7219$. Analysis of the La Jolla Nd standard yielded $^{143}Nd/^{144}Nd=0.511855\pm8$ (2-sigma error). Analytical blanks of Sm and Nd were always less than 0.03% of the elements processed from the samples. The new data, reported in Table 2, complement previous analyses from the Bhainskati and Dumri Formations in Nepal [6].

5.3. Trace element data

As discussed by [13] and references therein, Ni and Cr in mudrocks may be derived from breakdown of olivine and spinel, respectively, in mafic source rocks. Thus, in Himalayan Tertiary mudrocks, Ni and Cr concentrations are potential indicators of sediment sources in ophiolites and mafic igneous rocks of the Indus-Yarlung suture zone. Fifteen samples of mudrock from the Charchare, Bhainskati, and Dumri Formations were analyzed by X-ray fluorescence for Cr and Ni contents as a means of determining possible mafic suture zone detrital input. These data are reported in Table 3.

6. Results

6.1. Detrital zircon U–Pb ages

The Charchare Conglomerate and Amile Formation samples are characterized by zircon ages between 1450 and 3100 Ma, with the largest number of grains in the 1850–2550-Ma range (Fig. 4). As mentioned above, the Charchare sample yielded one grain with a mid-Cretaceous (125 Ma) age. In contrast, detrital zircons in the Bhainskati Formation fall into three age groups at ~500–800, ~1000–2100, and ~2400–3200 Ma. Two of the 343 Bhainskati grains analyzed produced mid-Cretaceous ages (102 and 122 Ma) and one grain produced an Early Triassic age (243 Ma). Detrital zircon ages in the Dumri Formation are broadly similar to those in the Bhainskati Formation, with the addition of a few grains in the 470–500-Ma range and an increased relative proportion of grains in the ~1000–1500-Ma range (Fig. 4).

6.2. Nd-isotopes

The Nd-isotopic data (Table 2) provide $\varepsilon_{Nd}(T)$ values of −6.2 to −14.4. The sample from the Charchare Conglomerate has $\varepsilon_{Nd}(T)=-6.2$. The Bhainskati samples have a mean $\varepsilon_{Nd}(T)$ value of −10.0, and the Dumri samples yielded a mean $\varepsilon_{Nd}(T)$ value of −14.4. The $\varepsilon_{Nd}(T)$ values from the new data are consistent with values reported by Robinson et al. [6], and the complete data set is plotted in Fig. 7.

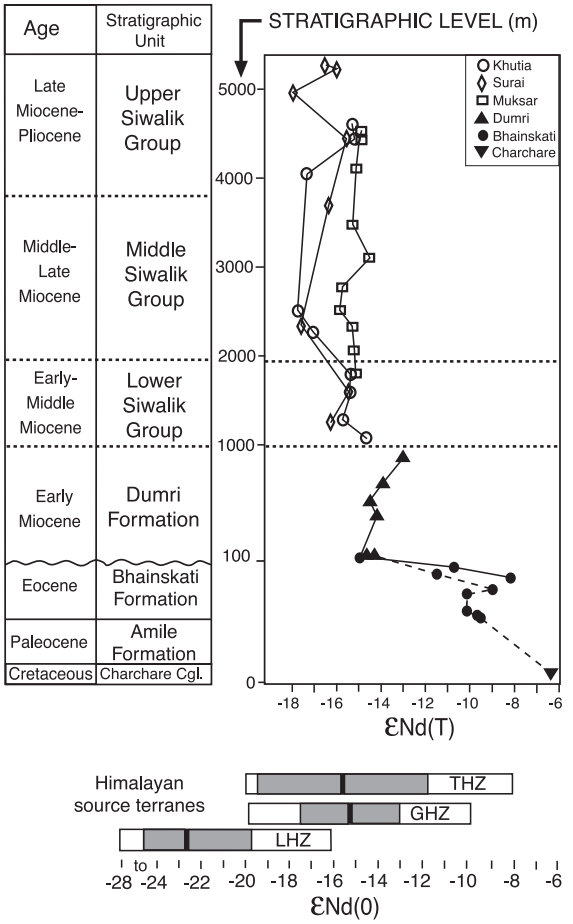

Fig. 7. Plot of $\varepsilon_{Nd}(T)$ values of fluvial and marine shales and siltstones from latest Cretaceous–Paleocene(?) through Early Miocene strata of the Nepalese Lesser Himalayan zone. Data reported in this paper are from the Charchare Conglomerate, Bhainskati Formation, and lower Dumri Formation. All other data are from [6]. Dashed line connects data reported herein.

Sample DB02-21KX, a siltstone interbedded within the Charchare Conglomerate, contains higher concentrations of Sm and Nd and has a lower Sm/Nd ratio than all other samples.

6.3. Trace element data

The Cr and Ni trace element data (Table 3) are plotted in Fig. 8. The Dumri Formation samples are generally very low in both Cr and Ni, whereas Bhainskati and Charchare Conglomerate samples yielded overlapping ranges of concentrations from 79–169 ppm Cr and 23–145 ppm Ni. Approximately half of the Bhainskati samples are significantly more enriched in Ni and Cr than North American Shale Composite (NASC), which is considered to be representative of continental upper crust [79]. All of the Dumri samples have low concentrations of Cr and Ni compared to NASC. A similar pattern was documented in roughly age-equivalent Eocene–Lower Miocene foreland basin deposits of northern India [13].

6.4. Bulk petrography and dense mineral data

Sandstones derived from orogenic terranes typically are rich in low- to medium-grade metasedimentary and sedimentary lithic grains (e.g., [1,80]). The bulk petrography of Amile and Bhainskati Formation sandstones is dominated by monocrystalline quartz (Fig. 3;

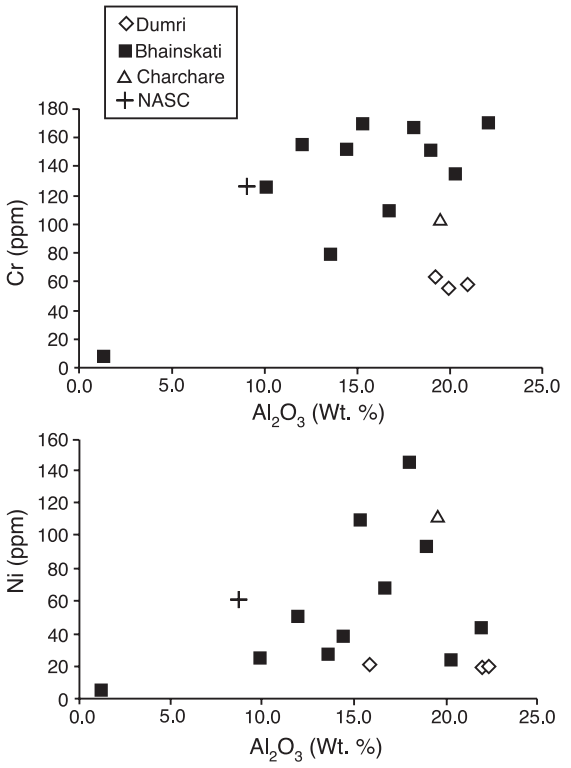

Fig. 8. X-ray fluorescence analyses of mudstone samples (see Table 3 and Fig. 5 for sample locations). NASC represents North American Shale Composite, which is taken as an average of upper continental crust [79].

[16]) and thus provides no definitive evidence for Himalayan erosion. Dumri sandstones contain abundant low-grade metasedimentary lithic grains and significant amounts of plagioclase. Dense minerals separated from the Amile Formation include tourmaline, zircon, rutile, titanium minerals, and traces of epidote, garnet and brown spinel. The Bhainskati Formation contains zircon, rutile, and significant reddish-brown spinel, with rare garnet.

7. Interpretation

The marked contrast in U–Pb zircon age distributions between the Amile and Bhainskati Formations is interpreted to be the result of the transition from a sediment source dominated by the northern Indian craton to one dominated by the growing Himalayan thrust belt. The transition occurs abruptly between sandstone samples at the 20- and 26-m levels of the section (Fig. 5). The pattern of ages in the Amile Formation and Charchare Conglomerate is reminiscent of the pattern exhibited by Lesser Himalayan rocks (Fig. 4), suggesting a source in the Early Proterozoic to Archean rocks of the Indian craton [65,66]. Most significantly, the Amile zircon age pattern shows no sign of derivation from Tethyan strata or Greater Himalayan rocks, which are characterized by Cambrian to Middle Proterozoic ages. The Bhainskati Formation shows a typical Tethyan zircon-age pattern, with significant numbers of 470–520 Ma grains that are generally not present in detrital zircons of the Greater Himalayan zone (Fig. 4). Conceivably, these Cambrian–Ordovician grains could have been derived from Formation III orthogneisses and related granites of the GHZ, but this is not supported by Nd-isotopic data (Fig. 7) that indicate Greater Himalayan rocks were not exposed until Miocene time [5,6,76]. In addition, the Albian (102 Ma) grain in the Bhainskati suggests a source in the Gangdese arc or Indus forearc region, where mid- to Late Cretaceous granitic rocks are widespread [68,69,82 and references therein]. The Dumri Formation has a detrital zircon age distribution that is similar to that of the Bhainskati Formation, with a greater relative proportion of Late Proterozoic grains possibly reflecting input from Greater Himalayan rocks by Early Miocene time.

The Nd isotopic data support previously published data [6] that indicate the Bhainskati Formation is more isotopically juvenile than the Dumri Formation. Together, the new and previously published Nd data manifest a general up-section decrease in $\varepsilon_{Nd}(T)$ values from the Charchare Conglomerate through the Siwalik Group (Fig. 7). By Early Miocene time, $\varepsilon_{Nd}(T)$ values in the foreland basin sediments were identical to values from the Greater Himalayan sequence. The Nd data suggest that the transition from southerly to northerly provenance can be isolated to the top of the Amile sandstone just above the 20-m level of the section (Figs. 5 and 7).

The trace element data provide evidence for sediment sources in mafic arc and ophiolitic rocks of the Indus-Yarlung suture zone during the Eocene part of the record. The highest concentrations of Cr and Ni are from samples located in the lower part of the Bhainskati Formation (below the ~80-m level in Fig. 5). The upsection decrease in Cr and Ni concentrations within the Bhainskati Formation is consistent with the detrital zircon U–Pb ages that indicate a predominance of sources in sedimentary rocks of the Tethyan sequence.

The simplest explanation of the provenance of the Cretaceous through lower Miocene strata is as follows:

(1) The Charchare Conglomerate and Amile Formation were derived from the northern Indian craton, with perhaps minor additions of detritus from the Cretaceous Rajmahal igneous province and/or related volcanic sources in northeastern cratonic India (Fig. 9). In the single Charchare sample analyzed for Nd, a low Sm/Nd ratio and high Sm and Nd concentrations are consistent with derivation from alkaline igneous rocks such as the widespread Early Cretaceous volcanics in northern peninsular India.

(2) Beginning in Early to Middle Eocene time, an influx of 500–1500 Ma zircons accompanied initial erosion of the rising Himalayan thrust belt, which at that time was composed entirely of Tethyan sedimentary rocks and Cretaceous igneous rocks in the Indus-Yarlung suture zone and forearc. The presence of Cr-spinel in the dense mineral fraction from the Bhainskati Formation is a diagnostic signal that the suture

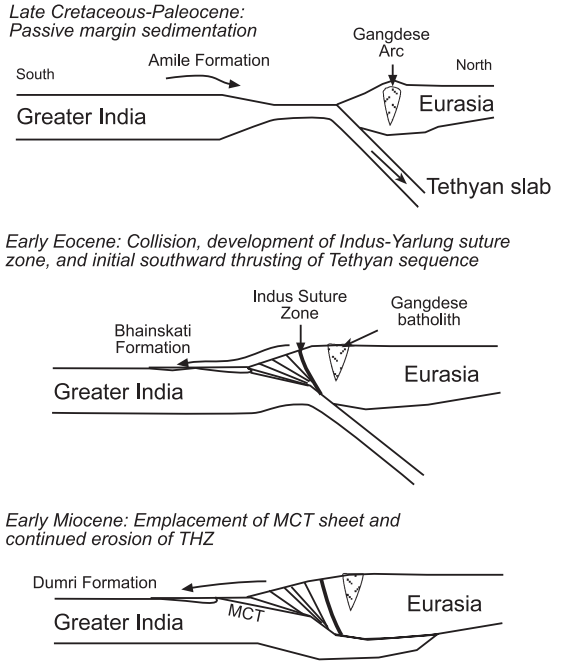

Fig. 9. Schematic cross sections showing the kinematic sequence responsible for the evolution of sediment provenance in the Himalayan foreland basin, based on data presented in this paper and previously published papers [5,6,13,16,41,59,76,83].

zone supplied some Bhainskati detritus [13]. The upsection decreases in Cr and Ni concentrations in the Bhainskati Formation coupled with a parallel decrease in $\varepsilon_{Nd}(T)$ values reflect temporally increasing Tethyan thrust belt sources at the expense of suture zone sources.

(3) By Early Miocene time, the fluvial deposits of the Dumri Formation were being derived from both Tethyan rocks and Greater Himalayan protoliths, as indicated by the increased proportion of ~1100 Ma grains and the persistence of ~500 Ma grains. A negative shift in $\varepsilon_{Nd}(T)$ values (from ~−11 to −15) in samples collected across the Bhainskati to Dumri transition supports the interpretation that Greater Himalayan protoliths in Nepal were not exposed until the Early Miocene [6,16]. A similar shift in $\varepsilon_{Nd}(T)$ values is recorded in Eocene to Early Miocene foreland basin deposits in northern India [83]. Moreover, petrographic data from Dumri Formation sandstones indicate a shift to relatively lithic- and plagioclase-rich compositions, suggesting sediment sources with Greater Himalayan affinity [16]. However, the lack of high-grade metamorphic lithic fragments in the Dumri precludes a significant source in the Greater Himalayan high-grade metamorphic rocks. Perhaps the slightly metamorphosed lower part of the Tethyan sequence, which is a likely candidate for Greater Himalayan protoliths [24,29,43], was a source of Dumri sandstones. Coupled with thermochronological constraints on the Early Miocene age of exhumation of the Greater Himalayan sequence (e.g., [47]), our provenance data suggest that the Dumri Formation was derived from lower Tethyan metasedimentary rocks during initial emplacement of the Main Central thrust sheet.

(4) Zircons from the Middle Miocene to Pliocene foreland basin deposits of the Siwalik Group and modern river sands in Nepal [16,41] exhibit an increase in the older age fraction (particularly the ~1800-Ma ages), reflecting the increase in availability of Lesser Himalayan zircons that coincided with deep erosion into the Lesser Himalayan duplex and emplacement of the Ramgarh and Main Boundary thrust sheets. However, Nd-isotopic data from the foreland basin deposits [5,6] and the Bengal fan [53,54] indicate that Greater Himalayan rocks have been the primary source of siliciclastic detritus since the Early Miocene.

The fact that detrital zircons in modern river sands [41,42] of known Himalayan provenance exhibit age patterns similar to those documented in the post-Amile Tertiary rocks adds robustness to the interpretation of Himalayan zircon provenance. Our provenance interpretation is consistent with independent constraints on the kinematic history of thrusting in the central part of the Himalayan thrust belt, which indicate a general southward progression of major thrusting events from the THZ to the Main Frontal thrust (see summaries in [9,59]).

8. Discussion and conclusions

Rowley [8,15] noted that the Eocene section at Zhepure Mountain (Fig. 1) in southern Tibet consists of shallow-marine carbonate and fine-grained clastic

rocks that lack evidence for rapid subsidence as expected for a basin in which thrust loading was the principal mechanism of flexural subsidence. This region is almost due north of our study area and therefore raises the question of how this apparently pre-orogenic section is related to the Eocene section in the Lesser Himalayan zone of Nepal, which we interpret to be synorogenic. We suggest that the Zhepure Mountain area lay on the crest of a shallow-marine flexural forebulge during Eocene time, while the study area in south-central Nepal lay in the back-bulge depositional zone of the foreland basin system [84]. Southward migration of the forebulge wave relative to Indian lithosphere produced the ~20-My disconformity between the Bhainskati and Dumri Formations. This disconformity can be traced throughout the entire Himalayan foreland basin system from eastern Nepal to western Pakistan (Fig. 2).

This model can be tested by combining elastic flexural models with an Eocene palinspastic reconstruction of the Himalayan thrust belt at the approximate latitude of our study area (Fig. 10). The most important control on the wavelength of flexural perturbation in a foreland basin system is the flexural rigidity (D) of the foreland lithosphere. Previous studies have shown that D for northern Indian lithosphere ranges between 3×10^{23} and 7×10^{24} N m [85,86]. It is likely that Indian lithosphere being subducted beneath Eurasia at the onset of the collision was considerably less rigid than present foreland

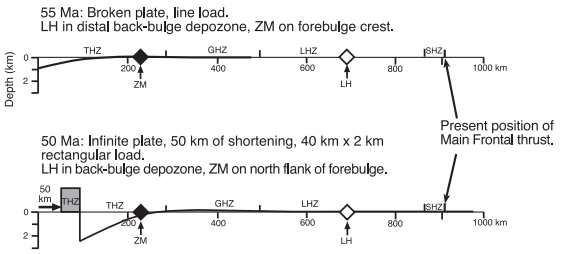

Fig. 10. Two-dimensional flexural models of the early Himalayan foreland basin system at the Lat. of central Nepal. Flexural rigidity is 1.5×10^{23} N m (corresponding to effective elastic thickness of 28.8 km). For the 55-Ma profile, a line load on a broken plate is used; for the 50-Ma profile a 40×2-km rectangular load flexes an infinite plate. The horizontal scale bar shows palinspastic locations of the Subhimalayan (SHZ), Lesser Himalayan (LHZ), Greater Himalayan (GHZ), and Tibetan Himalayan (THZ) zones; diamonds represent the restored locations of the Zhepure Mountain (ZM) and Lesser Himalayan (LH) Tertiary sections.

lithosphere in northern India. We therefore decrease the lower bound of D values to 1.5×10^{23} N m (a reasonable estimate for transitional oceanic lithosphere [87]). We illustrate flexural models for both broken and infinite flexed plates. For Eocene time, a broken plate is probably the most realistic, insofar as the Tethyan oceanic slab probably detached soon after initial collision [88]. The palinspastic reconstruction of the Himalayan thrust belt is based on regional balanced cross sections in Nepal [59] and southern central Tibet [22,23]. The results demonstrate that the Zhepure Mountain section could have been situated on the crest of the forebulge at the same time that the Lesser Himalayan Tertiary section was located in the back-bulge region. Isolated from clastic input by its elevated (but still submarine) position, the Zhepure Mountain area developed a carbonate platform, analogous to carbonate build-ups that occupy submarine forebulges in other collisional foreland regions (e.g., [84,89,90]).

The Cretaceous–Paleocene strata of southern Nepal were derived from the northern Indian shield and possibly Cretaceous volcanic rocks of northeastern India. Eocene strata were derived from recycled Tethyan sedimentary rocks that were exposed in the newly developed Himalayan thrust belt, with contributions from the Indus suture zone. By Early Miocene time, sediment derived from the Tethyan and Greater Himalayan zones began to accumulate in the fluvial Dumri Formation. In Nepal, therefore, the transition from Indian (southerly) to Himalayan (northerly) provenance can be pinpointed to the contact between the sandstone-rich Amile Formation and the overlying black shale-rich Bhainskati Formation. Although the exact age of this transition is not known because of ambiguities in Amile Formation biostratigraphy and the lack of age control in the lower part of the Bhainskati Formation, the change took place sometime before Middle Eocene time (>49 Ma). This implies that, unless significant along-strike transport of detritus occurred, the onset of Himalayan orogeny in Nepal was at most only slightly younger than it was in the Zanskar Himalaya to the northwest. Within the limits of the existing biostratigraphy, the maximum permissible lag time between the onset of orogeny in Zanskar [10] and Nepal is ~2 million years.

Finally, the data presented herein demonstrate the usefulness of a combined geochemical and geo-

chronological approach to assessing provenance in ultrastable, supermature sediments that lack conventional petrographic indicators of syndepositional tectonic activity. In this case, the Eocene sandstones of Nepal have ultrastable compositions because the region was situated at equatorial latitudes during deposition [16]. The durability of detrital zircons and stability of Nd isotopes even in the face of extreme weathering conditions [3] presents an ideal opportunity to assess provenance with isotopic methods.

Acknowledgments

We thank Alex Pullen for help with zircon sample processing, S. Andò and G. Vezzoli for assistance with point-counting and dense mineral analyses, and T.P. Ojha for logistical support. We gratefully acknowledge Jon Patchett and Clark Isachsen for their assistance in the Sm–Nd isotopic analyses. Reviews by M.P. Searle and E.J. Catlos helped us to substantially improve the manuscript. This work was supported by grants from the U.S. National Science Foundation (grant EAR-0207179 to DeCelles and Gehrels) and the Royal Society of Edinburgh (Najman).

Appendix A. Supplementary data

Supplementary data associated with this article can be found, in the online version, at doi:10.1016/j.epsl.2004.08.019.

References

[1] W.R. Dickinson, C.A. Suczek, Plate tectonics and sandstone composition, Am. Assoc. Pet. Geol. Bull. 63 (1979) 2164–2182.

[2] A.R. Basu, M. Sharma, P.G. DeCelles, Nd–Sr isotopic provenance and trace element geochemistry of Amazonian foreland-basin sands from Peru and Bolivia: implications for Andean ensialic orogenesis, Earth Planet. Sci. Lett. 100 (1990) 1–17.

[3] S.M. McLennan, S. Hemming, D.K. McDaniel, G.N. Hanson, Geochemical approaches to sedimentation, provenance, and tectonics, in: M.J. Johnsson, A. Basu (Eds.), Processes Controlling the Composition of Clastic Sediments, Geol. Soc. Am. Spec. Pap. 284 (1993) 21–40.

[4] J.D. Gleason, P.J. Patchett, W.R. Dickinson, J. Ruiz, Nd isotopes link Ouachita turbidites to Appalachian source, Geology 22 (1994) 347–350.

[5] N.M. White, M. Pringle, E. Garzanti, M. Bickle, Y. Najman, H. Chapman, P. Friend, Constraints on the exhumation and erosion of the high Himalayan slab, NW India, from foreland basin deposits, Earth Planet. Sci. Lett. 195 (2001) 29–44.

[6] D.M. Robinson, P.G. DeCelles, P.J. Patchett, C.N. Garzione, The kinematic history of the Nepalese Himalaya interpreted from Nd isotopes, Earth Planet. Sci. Lett. 192 (2001) 507–521.

[7] W.R. Dickinson, G.E. Gehrels, U–Pb ages of detrital zircons from Permian and Jurassic eolian sandstones of the Colorado Plateau, USA: paleogeographic implications, Sediment. Geol. 163 (2003) 29–66.

[8] D.B. Rowley, Age of initiation of collision between India and Asia: a review of stratigraphic data, Earth Planet. Sci. Lett. 145 (1996) 1–13.

[9] S. Guillot, E. Garzanti, D. Baratoux, D. Marquer, G. Mahéo, J. de Sigoyer, Reconstructing the total shortening history of the NW Himalaya, Geochem. Geophys. Geosyst. 4 (2003) DOI:10.1029/2002GC000484.

[10] S. Critelli, E. Garzanti, Provenance of the lower Tertiary Murree redbeds (Hazara-Kashmir syntaxis, Pakistan) and initial rising of the Himalayas, Sediment. Geol. 89 (1994) 265–284.

[11] D.A. Pivnik, N.A. Wells, The transition from Tethys to the Himalaya as recorded in northwest Pakistan, Geol. Soc. Am. Bull. 108 (1996) 1295–1313.

[12] E. Garzanti, S. Critelli, R.V. Ingersoll, Paleogeographic and paleotectonic evolution of the Himalayan Range as reflected by detrital modes of Tertiary sandstones and modern sands (Indus transect, India and Pakistan), Geol. Soc. Am. Bull. 108 (1996) 631–642.

[13] Y. Najman, E. Garzanti, Reconstructing early Himalayan tectonic evolution and paleogeography from Tertiary foreland basin sedimentary rocks, northern India, Geol. Soc. Am. Bull. 112 (2000) 435–449.

[14] H. Willems, Z. Zhou, B. Zhang, K.-U. Gräfe, Stratigraphy of the Upper Cretaceous and lower Tertiary strata in the Tethyan Himalaya of Tibet (Tingri area, China), Geol. Rundsch. 85 (1996) 723–754.

[15] D.B. Rowley, Minimum age of initiation of collision between India and Asia north of Everest based on the subsidence history of the Zhepure Mountain section, J. Geol. 106 (1998) 229–235.

[16] P.G. DeCelles, G.E. Gehrels, J. Quade, T.P. Ojha, Eocene–Early Miocene foreland basin development and the history of Himalayan thrusting, western and central Nepal, Tectonics 17 (1998) 741–765.

[17] H. Sakai, Geology of the Tansen Group of the Lesser Himalaya in Nepal, Mem. Fac. Sci., Kyushu Univ., D 25 (1983) 27–74.

[18] H. Sakai, The Gondwanas in the Nepal Himalaya, in: S.K. Tandon, C.C. Pant, S.M. Casshyap (Eds.), Sedimentary Basins of India: Tectonic Context, Gyanodaya Prakashan, Nainital, 1991, pp. 202–217.

[19] A. Gansser, Geology of the Himalayas, Wiley Interscience, London, 1964, 289 pp.
[20] J.P. Burg, G.M. Chen, Tectonics and structural zonation of southern Tibet, Nature 311 (1984) 219–223.
[21] M.P. Searle, R.I. Corfield, B. Stephenson, J. McCarron, Structure of the north Indian continental margin in the Ladakh-Zanskar Himalayas: implications for the timing of obduction of the Spontang ophiolite, India–Asia collision and deformation events in the Himalaya, Geol. Mag. 134 (1997) 297–316.
[22] L. Ratschbacher, W. Frisch, G. Liu, C. Chen, Distributed deformation in southern and western Tibet during and after the India–Asia collision, J. Geophys. Res. 99 (1994) 19917–19945.
[23] M.A. Murphy, A. Yin, Structural evolution and sequence of thrusting in the Tethyan fold–thrust belt and Indus-Yalu suture zone, southwest Tibet, Geol. Soc. Am. Bull. 115 (2003) 21–34.
[24] M. Colchen, P. LeFort, A. Pêcher, Annapurna-Manaslu-Ganesh Himal, Centre National de la Recherché Scientifique, Paris, 1986, 126 pp.
[25] G. Fuchs, R.W. Widder, R. Tuladhar, Contributions to the geology of the Annapurna Range (Manang area, Nepal), Jahrb. Geol. Bundesanst. 131 (1988) 593–607.
[26] M. Gaetani, E. Garzanti, Multicyclic history of the northern India continental margin (Northwestern Himalaya), Am. Assoc. Pet. Geol. Bull. 75 (1991) 1427–1446.
[27] M.E. Brookfield, The Himalayan passive margin from Precambrian to Cretaceous times, Sediment. Geol. 84 (1993) 1–35.
[28] E. Garzanti, Stratigraphy and sedimentary history of the Nepal Tethys Himalaya passive margin, J. Asian Earth Sci. 17 (1999) 805–827.
[29] A. Steck, Geology of the NW Indian Himalaya, Eclogae Geol. Helv. 96 (2003) 147–196.
[30] J. Lee, B.R. Hacker, W.S. Dinklage, Y. Wang, P. Gans, A. Calvert, J.L. Wan, W. Chen, A.E. Blythe, W. McClelland, Evolution of the Kangmar Dome, southern Tibet: structural, petrologic, and thermochronologic constraints, Tectonics 19 (2000) 872–895.
[31] B.C. Burchfiel, Z. Chen, K.V. Hodges, Y. Liu, L.H. Royden, C. Deng, J. Xu, The South Tibetan detachment system, Himalayan orogen: extension contemporaneous with and parallel to shortening in a collisional mountain belt, Geol. Soc. Am. Spec. Pap. 269 (1992) 41 pp.
[32] K.V. Hodges, R.R. Parrish, M.P. Searle, Tectonic evolution of the central Annapurna Range, Nepalese Himalayas, Tectonics 15 (1996) 1264–1291.
[33] P. Dèzes, J.-C. Vannay, A. Steck, F. Bussy, M. Cosca, Synorogenic extension; quantitative constraints on the age and throw of the Zanskar shear zone (NW Himalayas), Geol. Soc. Amer. Bull. 111 (1999) 364–374.
[34] A. Pêcher, The metamorphism in central Himalaya, J. Metamorph. Geol. 7 (1989) 31–41.
[35] M.P. Searle, L. Godin, The South Tibetan detachment and the Manaslu leucogranite: a structural reinterpretation and restoration of the Annapurna-Manaslu Himalaya, Nepal, J. Geol. 111 (2003) 505–523.
[36] J.-C. Vannay, K.V. Hodges, Tectonometamorphic evolution of the Himalayan metamorphic core between Annapurna and Dhaulagiri, central Nepal, J. Metamorph. Geol. 14 (1996) 635–656.
[37] J.R. Trivedi, K. Gopalan, K.S. Valdiya, Rb–Sr ages of granitic rocks within the Lesser Himalayan nappes, Kumaon, J. Geol. Soc. India 25 (1984) 641–654.
[38] P. LeFort, F. Debon, A. Pêcher, J. Sonet, P. Vidal, The 500 Ma magmatic event in Alpine southern Asia, a thermal episode at Gondwana scale, Sci. Terre, Mém. 47 (1986) 191–209.
[39] G. Ferrara, B. Lombardo, S. Tonarini, Rb/Sr geochronology of granites and gneisses from the Mount Everest region, Nepal Himalaya, Geol. Rundsch. 72 (1983) 119–136.
[40] U. Schärer, C.J. Allègre, The Palung granite (Himalaya): high resolution U–Pb systematics in zircon and monazite, Earth Planet. Sci. Lett. 63 (1983) 423–432.
[41] P.G. DeCelles, G.E. Gehrels, J. Quade, P.A. Kapp, T.P. Ojha, B.N. Upreti, Neogene foreland basin deposits, erosional unroofing, and the kinematic history of the Himalayan fold–thrust belt, western Nepal, Geol. Soc. Amer. Bull. 110 (1998) 2–21.
[42] P.G. DeCelles, G.E. Gehrels, J. Quade, B. LaReau, M. Spurlin, Tectonic implications of U–Pb zircon ages of the Himalayan orogenic belt in Nepal, Science 288 (2000) 497–499.
[43] G.E. Gehrels, P.G. DeCelles, A. Martin, T.P. Ojha, G. Pinhassi, B.N. Upreti, Initiation of the Himalayan orogen as an Early Paleozoic thin-skinned thrust belt, GSA Today 13 (2003) 4–9.
[44] M.E. Coleman, U–Pb constraints on Oligocene–Miocene deformation and anatexis within the central Himalaya, Marsyandi valley, Nepal, Am. J. Sci. 298 (1998) 553–571.
[45] T.M. Harrison, M. Grove, K.D. McKeegan, C.D. Coath, O.M. Lovera, P. Le Fort, Origin and episodic emplacement of the Manaslu intrusive complex, central Himalaya, J. Petrol. 40 (1999) 3–19.
[46] M.P. Searle, S.R. Noble, A.J. Hurford, D.C. Rex, Age of crustal melting, emplacement and exhumation history of the Shivling leucogranite, Garhwal Himalaya, Geol. Mag. 136 (1999) 513–525.
[47] K.V. Hodges, Tectonics of the Himalaya and southern Tibet from two perspectives, Geol. Soc. Am. Bull. 112 (2000) 324–350.
[48] R.R. Parrish, K.V. Hodges, Isotopic constraints on the age and provenance of the Lesser and Greater Himalayan sequences, Nepalese Himalaya, Geol. Soc. Amer. Bull. 108 (1996) 904–911.
[49] T. Ahmad, N. Harris, M. Bickle, H. Chapman, J. Bunbury, C. Prince, Isotopic constraints on the structural relationships between the Lesser Himalayan Series and the High Himalayan Crystalline Series, Garhwal Himalaya, Geol. Soc. Amer. Bull. 112 (2000) 467–477.
[50] A. Whittington, G. Foster, N. Harris, D. Vance, M. Ayres, Lithostratigraphic correlations in the western Himalaya—an isotopic approach, Geology 27 (1999) 585–588.

[51] D. Vance, M. Bickle, S. Ivy-Ochs, P.W. Kubik, Erosion and exhumation in the Himalaya from cosmogenic isotope inventories of river sediments, Earth Planet. Sci. Lett. 206 (2003) 273–288.
[52] A.J. Martin, P.G. DeCelles, P.J. Patchett, Differentiating between models of MCT evolution in the Annapurna Range, Central Nepal Himalaya, AGU Fall Meeting, San Francisco, Abstracts with Programs, p. 1142.
[53] A. Bouquillon, C. France-Lanord, A. Michard, J. Tiercelin, Sedimentology and isotopic chemistry of the Bengal fan sediments: the denudation of the Himalaya, Proc. Ocean Drill. Prog., Sci. Results 116 (1990) 43–58.
[54] C. France-Lanord, L. Derry, A. Michard, Evolution of the Himalaya since Miocene time: isotopic and sedimentological evidence from the Bengal fan, in: P.J. Treloar, M.P. Searle (Eds.), Himalayan Tectonics, Spec. Publ.-Geol. Soc. Lond., vol. 74, 1993, pp. 605–622.
[55] K.S. Valdiya, Proterozoic sedimentation and Pan-African geodynamic development in the Himalaya, Precambr. Geol. 74 (1995) 35–55.
[56] B.N. Upreti, Stratigraphy of the western Nepal Lesser Himalaya: a synthesis, J. Nepal Geol. Soc. 13 (1996) 11–28.
[57] P. Srivastava, G. Mitra, Thrust geometries and deep structure of the outer and lesser Himalaya, Kumaon and Garhwal (India): implications for evolution of the Himalayan fold-and-thrust belt, Tectonics 13 (1994) 89–109.
[58] M.R.W. Johnson, Culminations and domal uplifts in the Himalaya, Tectonophysics 239 (1994) 139–147.
[59] P.G. DeCelles, D.M. Robinson, J. Quade, P. Copeland, B.N. Upreti, T.P. Ojha, C.N. Garzione, Regional structure and stratigraphy of the Himalayan fold–thrust belt, farwestern Nepal, Tectonics 20 (2001) 487–509.
[60] D.M. Robinson, P.G. DeCelles, C.N. Garzione, O.N. Pearson, T.M. Harrison, E.J. Catlos, Kinematic model for the Main Central thrust in Nepal, Geology 31 (2003) 359–362.
[61] J. Quade, J.M.L. Cater, T.P. Ojha, J. Adam, T.M. Harrison, Late Miocene environmental change in Nepal and the northern Indian subcontinent: stable isotopic evidence from paleosols, Geol. Soc. Amer. Bull. 107 (1995) 1381–1397.
[62] S. Singh, M.E. Barley, S.J. Brown, A.K. Jain, R.M. Manickavasagam, SHRIMP U–Pb in zircon geochronology of the Chor granitoid: evidence for Neoproterozoic magmatism in the Lesser Himalayan granite belt of NW India, Precambrian Res. 118 (2002) 285–292.
[63] H.C. Einfalt, A. Hoehndorf, K.P. Kaphle, Radiometric age determination of the Dadeldhura granite, Lesser Himalaya, Far Western Nepal, Schweiz. Mineral. Petrogr. Mitt. 73 (1993) 97–106.
[64] L. Godin, R.R. Parrish, R.L. Brown, K.V. Hodges, Crustal thickening leading to exhumation of the Himalayan metamorphic core of central Nepal: insight from U–Pb geochronology and $^{40}Ar/^{39}Ar$ thermochronology, Tectonics 20 (2001) 729–747.
[65] S.M. Naqvi, J.J.W. Rogers, Precambrian Geology of India, Clarendon Press, New York, 1987, 223 pp.
[66] A.M. Goodwin, Principles of Precambrian Geology, Academic Press, London, 1996, 327 pp.
[67] R.W. Kent, M.S. Pringle, R.D. Müller, A.D. Saunders, N.C. Ghose, $^{40}Ar/^{39}Ar$ Geochronology of the Rajmahal Basalts, India, and their relationship to the Kerguelen Plateau, J. Petrol. 43 (2002) 1141–1153.
[68] F. Debon, P. LeFort, S.M. Sheppard, J. Sonet, The four plutonic belts of the Transhimalaya–Himalaya: a chemical, mineralogical, isotopic, and chronological synthesis along a Tibet–Nepal section, J. Petrol. 27 (1986) 219–250.
[69] L. Ding, P. Kapp, D. Zhong, W. Deng, Cenozoic volcanism in Tibet: evidence for a transition from oceanic to continental subduction, J. Petrol. 44 (2003) 1833–1865.
[70] H. Sakai, Rifting of the Gondwanaland and uplifting of the Himalayas recorded in Mesozoic and Tertiary fluvial sediments in the Nepal Himalayas, in: A. Taira, F. Masuda (Eds.), Sedimentary Facies in the Active Plate Margin, Terra Science, Tokyo, 1989, pp. 723–732.
[71] A.K. Baksi, Petrogenesis and timing of volcanism in the Rajmahal flood basalt province, northeastern India, Chem. Geol. 121 (1995) 73–90.
[72] M.F. Coffin, M.S. Pringle, R.A. Duncan, T.P. Gladczenko, M. Storey, R.D. Müller, L.A. Gahagan, Kerguelen, hotspot magma output since 130 Ma, J. Petrol. 43 (2002) 1121–1139.
[73] H. Sakai, R. Hamamoto, K. Arita, Radiometric ages of alkaline volcanic rocks from the upper Gondwana of the Lesser Himalayas, western central Nepal and their tectonic significance, Bull. Dept. Geol., Tribhuvan Univ., Kathmandu, Nepal 2 (1992) 65–74.
[74] G. Fuchs, W. Frank, Geological investigations in west Nepal and their significance for the geology of the Himalayas, Geol. Rundsch. 59 (1970) 552–580.
[75] N.S. Mathur, Biostratigraphic aspects of the Subathu Formation, Kumaon Himalaya, Recent Res. Geol. 5 (1980) 96–112.
[76] Y.M.R. Najman, M.S. Pringle, M.R.W. Johnson, A.H.F. Robertson, J.R. Wijbrans, Laser $^{40}Ar/^{39}Ar$ dating of single detrital muscovite grains from early foreland-basin sedimentary deposits in India: implications for early Himalayan evolution, Geology 25 (1997) 535–538.
[77] J.S. Stacey, J.D. Kramers, Approximation of terrestrial lead isotope evolution by a two-stage model, Earth Planet. Sci. Lett. 26 (1975) 207–221.
[78] P.J. Patchett, J. Ruiz, Nd isotopic ages of crust formation and metamorphism in the Precambrian of eastern and southern Mexico, Contrib. Mineral. Petrol. 96 (1987) 523–528.
[79] L.P. Gromet, R.F. Dymek, L.A. Haskin, R.L. Korotov, The "North American Shale Composite": its compilation, major and trace element characteristics, Geochim. Cosmochim. Acta 48 (1984) 2469–2482.
[80] E. Garzanti, G. Vezzoli, A classification of metamorphic grains in sands based on their composition and grade, J. Sediment. Res. 73 (2003) 830–837.
[81] K.R. Ludwig, Isoplot/Ex, rev. 2.49: Berkeley geochronology center, Spec. Pub. 1A (2001) 56 pp.
[82] A. Yin, T.M. Harrison, Geologic evolution of the Himalayan–Tibetan orogen, Annu. Rev. Earth Planet. Sci. 28 (2000) 211–280.

[83] Y. Najman, M. Bickle, H. Chapman, Early Himalayan exhumation: isotopic constraints from the Indian foreland basin, Terra Nova 12 (2000) 28–34.
[84] P.G. DeCelles, K.N. Giles, Foreland basin systems, Basin Res. 8 (1996) 105–123.
[85] H. Lyon-Caen, P. Molnar, Gravity anomalies, flexure of the Indian plate, and the structure, support and evolution of the Himalaya and Ganga basin, Tectonics 4 (1985) 513–538.
[86] Y. Duroy, A. Farah, R.J. Lillie, Reinterpretation of the gravity field in the Himalayan foreland of Pakistan, in: L.L. Malinconico, R.J. Lillie (Eds.), Tectonics of the Western Himalayas, Geol. Soc. Am. 132 (1989) 217–236.
[87] D.L. Turcotte, G. Schubert, Geodynamics, 2nd ed., Cambridge Univ. Press, Cambridge, UK, 2002, 456 pp.
[88] A.I. Chemenda, J.-P. Burg, M. Mattauer, Evolutionary model of the Himalaya–Tibet system: geopoem based on new modelling, geological and geophysical data, Earth Planet. Sci. Lett. 174 (1999) 397–409.
[89] D.J. Pigram, P.J. Davies, D.A. Feary, P.A. Symonds, Tectonic controls on carbonate platform evolution in southern Papua New Guinea: passive margin to foreland basin, Geology 17 (1989) 199–202.
[90] S.L. Dorobek, Synorogenic carbonate platforms and reefs in foreland basins: controls on stratigraphic evolution and platform/reef morphology, in: S.L. Dorobek, G.M. Ross (Eds.), Stratigraphic Evolution of Foreland Basins, Spec. Pub. SEPM, vol. 79, 1995, pp. 127–147.
[91] K. Amatya, B. Jnawali, Geological Map of Nepal. DMG/ICIMOD/DCG/UNEP, 1994, scale 1:1,000,000.